Research Paper
J. Astron. Space Sci. 36(4), 265-281 (2019)
https://doi.org/10.5140/JASS.2019.36.4.265

JASS Journal of Astronomy and Space Sciences

UY Ursae Majoris: An A-Subtype W UMa System with a Very Large Fill-Out Factor and an Extreme Mass Ratio

Chun-Hwey Kim[1†], Mi-Hwa Song[1], Jang-Ho Park[1,2], Min-Ji Jeong[1], Hye-Young Kim[1], Cheongho Han[3]

[1]Department of Astronomy and Space Science, Chungbuk National University, Cheongju 28644, Korea
[2]Korea Astronomy and Space Science Institute, Daejeon 34055, Korea
[3]Department of Physics, Chungbuk National University, Cheongju 28644, Korea

We present new *BVRI* light curves of UY UMa with no O'Connell effect and a flat bottom secondary eclipse. Light curve synthesis with the Wilson-Devinney code gives a new solution, which is quite different from the previous study: UY UMa is an A-subtype over-contact binary with a small mass ratio of $q = 0.21$, a high inclination of 81°.4, a small temperature difference of $\Delta T = 18°$, a large fill-out factor of $f = 0.61$, and a third light of approximately 10% of the total systemic light. The absolute dimensions were newly determined. Seventeen new times of minimum light have been calculated from our observations. The period study indicates that the orbital period has intricately varied in a secular period increase in which two cyclical terms with periods of $12^{y}.0$ and $46^{y}.3$ are superposed. The secular period increase was interpreted to be due to a conservative mass transfer of 2.68×10^{-8} $M_{\odot}$/yr from the less massive to the more massive star. The cyclical components are discussed in terms of double-light time contributions from two additional bound stars. The statistical relations of Yang & Qian (2015) among the physical parameters of 45 deep, low mass ratio contact binaries were revisited by using the physical parameters of UY UMa and 25 Kepler contact binaries provided by Şenavci et al. (2016).

Keywords: contact binaries, UY Ursae Majoris, fundamental parameters, evolution status

1. INTRODUCTION

The light variability of UY UMa (2MASS J13443683 + 5513184, NSVS 2684105, SVS 359, UCAC4 727-048578) was discovered by S. Beljawsky in 1933 on a Simeiz plate (Guthnick & Prager 1934). In the same year, M. Zverev correctly classified it as an W UMa eclipsing binary and determined its light elements ($Min.I$ = HJD 2427307.49 + $0^{d}.37785E$; Guthnick & Prager 1934). Guthnick & Prager (1934) gave the photographic maximum and minimum magnitudes of the system as $11^{m}.5$ and $12^{m}.0$, respectively. Subsequently, the system was neglected for over 60 years until the first CCD *BV* photometric observations were made and analyzed by Yang et al. (2001, hereafter, YLL). YLL presented the *BV* light curves, showing partial eclipses at both eclipses and an O'Connell effect with Max. I approximately $0^{m}.03$ brighter than Max. II. Through their light curve analysis, YLL found that UY UMa is a W-subtype contact binary with an extremely small mass ratio of $q = 0.134$, a low inclination of 73°.4, a large temperature difference of $\Delta T = 414°$, and a small fill-out factor of $f = 0.053$. The O'Connell effect in the light curves was explained by a cool spot model on the more massive component. In addition, by using sixteen photoelectric times of minimum light with a time-span of only four years from 1995 to 1999, available to them at that time, they showed that the orbital period of UY UMa seems to be constant during the four-year time span. Recently, a period study of the system was made by Yu et al. (2017) who analyzed a total of 76 times of minimum light available to them. They suggested that the orbital period has varied in a cycli-

Received 8 NOV 2019 **Revised** 26 NOV 2019 **Accepted** 27 NOV 2019
†**Corresponding Author**
Tel: +82-43-261-3139, E-mail: kimch@chungbuk.ac.kr
ORCID: https://orcid.org/0000-0001-8591-4562

cal variation with a period of $14^{y}.26$ and a semi-amplitude of $0^{d}.0026$, which is superposed on a secularly increasing period at a rate of $\frac{dP}{dt} = +2.545 \times 10^{-7}$ d/yr. They interpreted that the secular increase in period was caused by mass transfer from the less massive to the more massive star, while the cyclical change in period could be caused by either magnetic activities of the components or a light time effect (LITE) due to an unseen tertiary body. Unfortunately, YLL and Yu et al. did not include earlier photographic timings given by S. Beljawsky and M. Zverev (Kreiner et al. 2001), with which one would see more clearly the long-term behavior of the secular period change of the system. No radial velocity curves were available, although numerous eclipse timings have been reported. Because there are no further studies of UY UMa since the studies of YLL and Yu et al., we included UY UMa in our observing programs of close binary stars with a view to confirming and/or improving the photometric results of YLL and Yu et al.

In this paper we present new CCD *BVRI* light curves of UY UMa with a long duration of totality at the secondary eclipse, which are totally different from YLL's light curves, thus, give quite different astrophysical parameters from those of YLL. Based on all available times of minimum light with a timespan longer than Yu et al., which include earlier timings as well as new ones, we also present a period study which gives a new dynamical picture of the system. Finally, based on our photometric results, we discuss the evolutionary status of UY UMa together with other overcontact binaries similar to UY UMa.

2. OBSERVATION AND NEW LIGHT CURVES

2.1 Observations

New *BVRI* observations of UY UMa were made on nine nights during February and March, 2008 with the 1.0-m reflector at the Mt. Lemmon Optical Astronomy Observatory (LOAO) in Arizona, USA. Since its establishment in 2003, the telescope has been remotely controlled at the Korea Astronomy and Space Science Institute (KASI) in Korea. An FLI IMG4301E CCD camera with a 22′.5 × 22′.5 field of view was electronically cooled during the observations. The standard *BVRI* filters were used. Each of the frames was 2 × 2 binned and differently exposed from 20 s to 30 s, suitable to UY UMa, according to the filters used and weather conditions of each night. UCAC4 727-048577 and UCAC4 726-049111 were chosen as the comparison and check stars, respectively. Our comparison star is the star used as a check star by YLL. Fig. 1 shows a finding chart of UY UMa with the comparison (marked as 'C') and check ('K') stars. The star (GSC 3854-0013, UCAC4 726-049104) marked as 'CY' in the

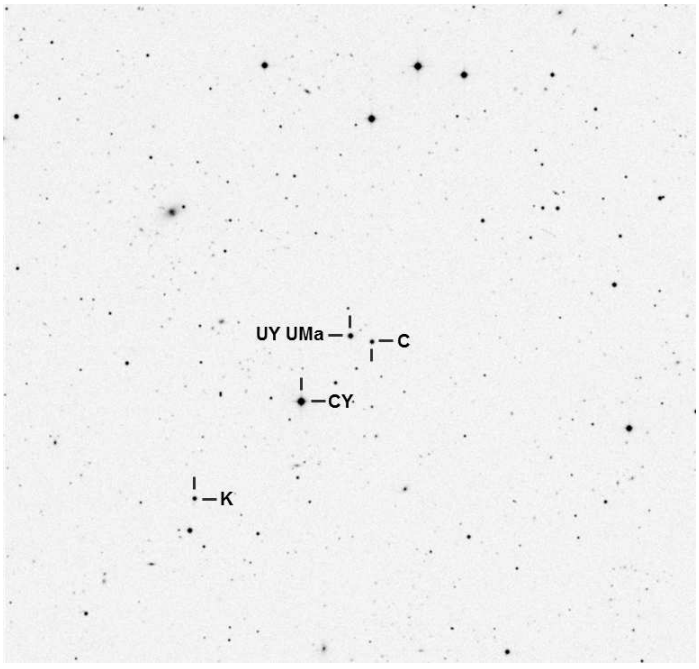

Fig. 1. The finding chart of UY UMa. The field of view is approximately 23′ × 23′. 'C' and 'K' denote the comparison (UCAC4 727-048577) and check (UCAC4 726-049111) stars, respectively. 'CY' denotes the comparison star (UCAC4 726-049104) used by Yang et al. (2001).

figure was YLL's comparison star, which is approximately seven and sixteen times brighter in yellow bandpass than UY UMa at the 0.25 phase and our comparison (and also check) star, respectively. Therefore, during our observations, the images taken in all bandpasses for the comparison star of YLL were always saturated at the camera exposure times of UY UMa. Table 1 lists the information on the coordinates, magnitudes, and color indices of the variable, comparison, and check stars.

The IRAF S/W package (Tody 1986) was used to reduce all measured frames with the conventional corrections of bias, dark, and flat-field. More details of our data reduction were described by Jeong & Kim (2013) and Kim et al. (2014). The resultant standard errors of our observations were approximately $\pm0^{m}.011$ in blue, $\pm0^{m}.020$ in yellow, and $\pm0^{m}.015$ in red, and $\pm0^{m}.020$ in infrared. A total of 2,976 individual observations were obtained in four colors (727 in blue, 761 in yellow, 782 in red, and 706 in infrared). Table 2 lists a sample of our measurements.

In addition to these observations, the *R* observations only for the determinations of times of minima were made for eight nights in 2009 at the LOAO and for one night in 2015 with an FLI 4K CCD camera attached to the 61-cm reflector at the Sobaeksan Optical Astronomy Observatory (SOAO) of the KASI in Korea. The instrumentation used and the reduction process for the LOAO observations are the same as those for the 2008 observations described above and the detail of the SOAO observations is well described in the paper of Kim et al. (2017).

2.2 New Light Curves

To phase our light curves, a linear least squares fit to 30 recent times of minima was made to yield the ephemeris:

$$Min.I = \text{JD Hel } 2451247.3267(6) + 0^{d}.37602172(6)E, \quad (1)$$

where the parenthesized figures give the standard errors of the last digit of each parameter. Fig. 2(a) shows the new *BVRI* light curves including the first *RI* ones. For comparison of our light curves with those of YLL, YLL's *BV* light curves were also drawn in Fig. 2(b). The differential color curves of $B - V$, $V - R$, and $R - I$ were calculated from our filtered light curves and shown in Fig. 2(c). In addition, the differential magnitudes at four characteristic phases and eclipse-depth information are listed in Table 3.

As seen in Fig. 2(a) and 2(b), our light curves are quite different from those of YLL in three ways: 1) The light curves of YLL show strong asymmetries, the so-called O'Connell effect (the light level at phase 0.25 is higher than that at phase 0.75; O'Connell 1951), while ours are nearly symmetrical, showing no O'Connell effect. Such light changes are typical to W UMa-type binary stars and have been usually interpreted as results of stellar activities

Table 1. Coordinates and photometric data for the program stars

Star	UCAC4	RA (J2000)	DEC (J2000)	V†	(B – V) †
UY UMa	727-048578	$13^{h}44^{m}36^{s}.83$	+55°13′18″.4	$+12^{m}.84$	$+0^{m}.58$
Comparison	727-048577	$13^{h}44^{m}31^{s}.88$	+55°13′06″.3	$+13^{m}.82$	$+0^{m}.75$
Check	726-049111	$13^{h}45^{m}13^{s}.32$	+55°07′56″.6	$+13^{m}.99$	$+0^{m}.98$
CY‡	726-049104	$13^{h}44^{m}48^{s}.45$	+55°11′09″.7	$+10^{m}.70$	$+0^{m}.64$

† From the UCAC4 Catalogue (Zacharias et al. 2013).
‡ Comparison star used by Yang et al. (2001).

Table 2. CCD *BVRI* photometric observations of UY UMa

HJD (day)	Δ*B* (mag)	HJD (day)	Δ*V* (mag)	HJD (day)	Δ*R* (mag)	HJD (day)	Δ*I* (mag)
2,454,508.8274	–1.291	2,454,508.8284	–1.131	2,454,508.8289	–1.066	2,454,508.8320	–0.995
2,454,508.8301	–1.309	2,454,508.8311	–1.151	2,454,508.8316	–1.068	2,454,508.8346	–1.000
2,454,508.8328	–1.299	2,454,508.8338	–1.144	2,454,508.8342	–1.075	2,454,508.8395	–0.987
2,454,508.8378	–1.310	2,454,508.8387	–1.149	2,454,508.8392	–1.072	2,454,508.8420	–0.994
2,454,508.8403	–1.310	2,454,508.8412	–1.160	2,454,508.8417	–1.087	2,454,508.8446	–1.005
2,454,508.8454	–1.325	2,454,508.8437	–1.154	2,454,508.8442	–1.092	2,454,508.8471	–0.997
2,454,508.8479	–1.312	2,454,508.8462	–1.171	2,454,508.8467	–1.091	2,454,508.8496	–1.003
2,454,508.8503	–1.324	2,454,508.8487	–1.159	2,454,508.8492	–1.071	2,454,508.8541	–0.990
2,454,508.8549	–1.326	2,454,508.8534	–1.152	2,454,508.8538	–1.080	2,454,508.8564	–0.985
2,454,508.8571	–1.321	2,454,508.8556	–1.157	2,454,508.8561	–1.077	2,454,508.8587	–0.985
2,454,508.8594	–1.311	2,454,508.8579	–1.149	2,454,508.8583	–1.096	2,454,508.8611	–0.983

This table is available at the web page (http://binary.cbnu.ac.kr/bbs/zboard.php?id=lab photometry). A portion is shown here for guidance regarding its form and content.

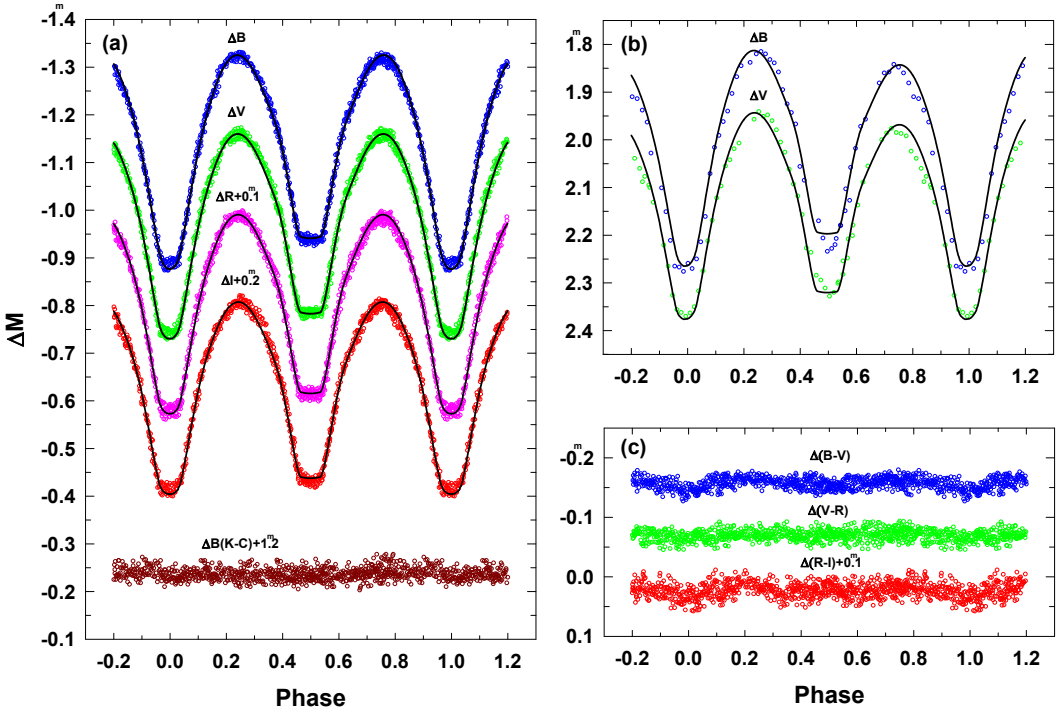

Fig. 2. (a) From top to bottom, *BVRI* differential light curves of UY UMa and *B* differential light curve of the check star. The solid curves represent the theoretical light curves calculated with our photometric solution in section 3. (b) YLL's *BV* differential light curves of UY UMa. The solid curves denote the theoretical light curves calculated with our solution and the spot parameters of YLL. (c) $B-V$, $V-R$, and $R-I$ differential color curves of UY UMa.

Table 3. Differential magnitudes and eclipse depths of UY UMa at four characteristic phases

Phase	ΔB (mag)	ΔV (mag)	ΔR (mag)	ΔI (mag)	Eclipse depth†			
					B (mag)	V (mag)	R (mag)	I (mag)
0.00	−0.890	−0.740	−0.680	−0.614	0.434	0.4190	0.410	0.393
0.25	−1.324	−1.159	−1.090	−1.007	–	–	–	–
0.50	−0.938	−0.785	−0.712	−0.632	0.386	0.3740	0.378	0.375
0.75	−1.318	−1.158	−1.086	−1.003	-	-	-	-

† Values for eclipse depth are relative to the phase 0.25.

such as cool or hot starspot(s) and their time variations. 2) Our light curves clearly have a flat-bottom at the secondary eclipse with a mean duration of approximately 43 min corresponding to an approximate 0.085 phase interval, while YLL's do not show any evidence of total eclipse at secondary eclipse. Initially, we were surprised at the morphological disagreement between two sets of light curves because our light curves indicate that UY UMa belongs to the A-subtype group of W UMa binaries rather than the W-subtype suggested by YLL, according to the criteria introduced by Binnendijk (1970). 3) Our light curves are approximately twelve times more dense in measurements than those of YLL; each of our light curves has over 85 measurements during the total eclipse at the secondary eclipse while each of YLL's blue and yellow light curves has only seven points for the same eclipse.

The apparent disagreement between our light curves and those of YLL may suggest that UY UMa had intrinsically changed from the W-subtype to the A-subtype or the photometry of YLL was not of adequate quality. The latter rather than the former may be the cause of the disagreement based on the reasoning as follows: 1) The comparison star used by YLL, seven times brighter in the V bandpass than UY UMa, is not properly chosen. 2) The measurements defining YLL's light curves are not sufficiently dense to distinguish the total eclipse at the secondary eclipse. A similar situation can also be found in the observational history of the A-subtype contact binary, V432 Per (see the papers of Yang & Liu 2002; Lee et al. 2008, Odell et al. 2009).

3. LIGHT CURVE SYNTHESIS

As previously noted, our *BVRI* light curves show a total occultation eclipse at secondary minimum, implying that UY UMa is an A-subtype W UMa contact binary. Simultaneous analysis of the multi-band light curves was made to obtain a unique solution with the 2003 version of the Wilson-Devinney (WD) differential corrections computer code (Wilson & Devinney 1971; Wilson 1979, 1990; van Hamme & Wilson 2003) which is available from ftp://ftp.astro.ufl.edu/pub/wilson/. To explain the total eclipse at the secondary minimum, the primary star (star 1) of UY UMa should be hotter, larger, and more massive than the secondary companion (star 2) and is being eclipsed at primary eclipse. The effective temperature of the primary star (T_1) is adopted as 5,900 K, corresponding to the (B – V) color index of 0.61 at phase 0.25 given by YLL (see also Drilling & Landolt 2000).

The temperature was fixed in our q-search procedure to deduce a most probable mass ratio q (= m_2/m_1) of UY UMa. The q-search without any surface perturbations such as any spot (s) or a third light (l_3) was intensively made for a series of models with the mass ratios varying from 0.1 to 1.0 at intervals of 0.01. In these searches, the gravity darkening exponents and bolometric albedos were set to 0.32 and 0.5 for both components, respectively, because both component stars are cool and are assumed to have convective envelopes. Logarithmic limb-darkening (LD) coefficients and bolometric LD coefficients for the primary and secondary stars were computed at each iteration from the LD tables given by Van Hamme (1993). The options of synchronous rotation and model atmosphere (Kurucz 1993) in the WD program were also adopted. All observations in each of the *BVRI* bandpasses were weighted equally. The adjustable parameters were the phase shift (ϕ), the orbital inclination (i), the effective temperature of the cooler component (T_2), the surface equipotential of both components ($\Omega = \Omega_1 = \Omega_2$), and the luminosity of the hotter primary component (l_1) in each of the bandpasses. The WD mode 3 for a contact system was adopted to adjust the parameters of UY UMa. Each of the fits converged rapidly. The result of our q search is shown in Fig. 3, where the abscissa is the mass ratio q and the ordinate is the weighted sum of squared residuals ($\Sigma W\,(O - C)^2$; hereafter, Σ). A global minimum of Σ occurred at q = 0.28, as indicated by the arrow in Fig. 3. At this point a third light was considered and adjusted with the other parameters above including the mass ratio. In this procedure, the method of multiple subsets (Wilson & Biermann 1976) was used to enhance the stability of the fit. The final solution is listed in Table 4,

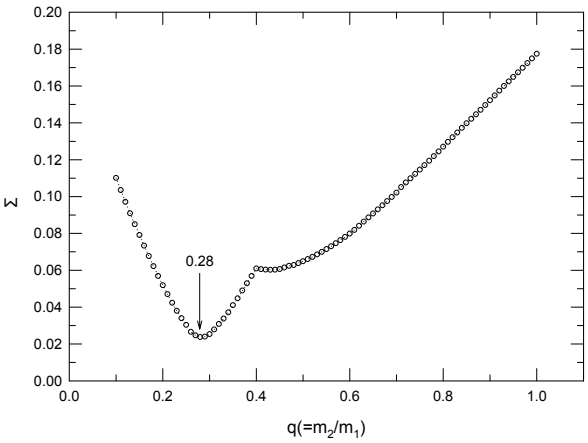

Fig. 3. q-search diagram of UY UMa. The arrow indicates the global minimum of $\Sigma W(O-C)^2$ at q = 0.28.

together with the YLL's solution for comparison. The *BVRI* residuals of the observations from our solution are shown in Fig. 4. The theoretical light curves calculated with our solution are drawn as solid curves in Fig. 2(a). The solid curves in Fig. 2(b) represent the theoretical light curves calculated with our solution plus the spot parameters of YLL. As shown in Figs. 2 and 4, our solution shows a fairly good representation of the observed multiband light curves within the observational errors.

As listed in Table 4, our solution is quite different in many respects from the one suggested by YLL. Our solution shows that UY UMa is an A-subtype over-contact binary with an extreme mass ratio of q = 0.21, a high inclination of 81°.4, a small temperature difference of ΔT = 18°, a large fill-out factor of f = 0.61, and a large third light amounting to approximately 10% of the total systemic light in the B bandpass. On the contrary, YLL's solution indicates that UY UMa is a W-subtype contact binary with an extremely small mass ratio of q = 0.134, a low inclination of 73°.4, a large temperature difference of ΔT = 414°, and a very small fill-out factor of f = 0.053. We believe that the serious disagreement between our solution and that of YLL may be due to their analysis of the light curves obtained from YLL's inadequate photometry rather than the real dramatic changes of the system parameters of UY UMa. Based on our photometric solution of UY UMa, the Roche geometry at phase 0.75 is shown in Fig. 5.

Since the radial velocity curve of UY UMa is not yet available, it is not possible to directly determine the absolute parameters of the binary system. However, it is well known that the mass ratio obtained from light curve syntheses is very reliable only for eclipsing systems with total eclipse such as in the case of UY UMa (Terrell & Wilson 2005; Hambalek & Pribulla 2013; Şenavci et al. 2016).

Table 4. Photometric parameters of UY UMa

Parameter	Yang et al. (2001)		This paper	
	Component 1	Component 2	Component 1	Compnent 2
q (= m_2 / m_1)	0.1331 (6)		0.2055 (8)	
i (°)	73.38 (41)		81.35 (18)	
$\Omega_1 = \Omega_2$	2.0515 (22)		2.167 (2)	
Fill-out factor	0.053		0.609	
T (K)	5,486 (12)	5,900†	5,900†	5,882 (4)
$l / (l_1 + l_2)_b$	0.7928 (10)	0.2072	0.7968 (9)	0.2032 (9)
$l / (l_1 + l_2)_v$	0.7805 (11)	0.2195	0.7962 (8)	0.2038 (8)
$l / (l_1 + l_2)_r$			0.7956 (8)	0.2044 (8)
$l / (l_1 + l_2)_i$			0.7957 (8)	0.2043 (8)
l_{3b}‡	-		0.106 (4)	
l_{3v}‡	-		0.084 (4)	
l_{3r}‡	-		0.063 (4)	
l_{3i}‡	-		0.052 (4)	
r (pole)	0.5357 (5)	0.2310 (6)	0.5043 (2)	0.2566 (6)
r (side)	0.5998 (8)	0.2441 (7)	0.5552 (2)	0.2704 (8)
r (back)	0.6263 (9)	0.3219 (13)	0.5845 (3)	0.3308 (10)
r (volume)	-	-	0.5488 (3)	0.2848 (8)
Spot				
ϕ (deg)	96.6 (2)	-	-	-
l (deg)	278.9 (2.9)	-	-	-
R (deg)	13.3 (3)	-	-	-
τ (= T_{spot} / T_{local})	0.84 (2)	-	-	-

† Fixed parameter.
‡ Value at 0.25 phase.

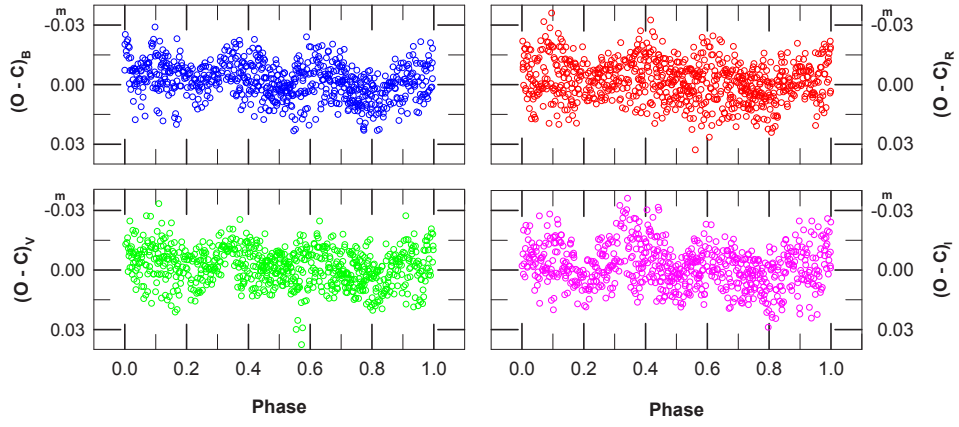

Fig. 4. *BVRI* residuals of the observations from the binary model in Table 4.

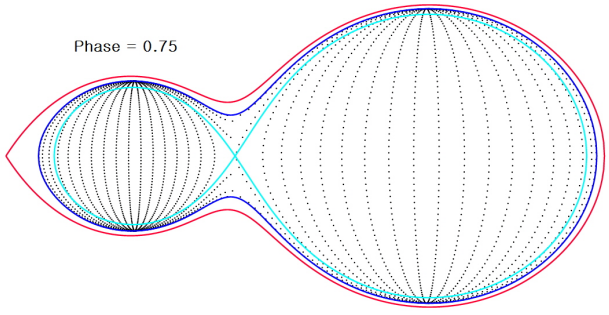

Fig. 5. Roche geometry of UY UMa at phase 0.75.

Thanks to this fact, we further pursued the absolute physical parameters of UY UMa by using the adopted light-curve parameters in Table 4 and some well-established relations, as described in detail in Kim et al. (2014).

The absolute dimensions and radiative parameters with their uncertainties were listed in Table 5 where the well-known calibrations (Flower 1996; Torres et al. 2010) were used to obtain the intrinsic color indices and bolometric corrections for the primary and secondary components and the distance was estimated with the assumption of no interstellar absorption. Our distance matches well with

Table 5. Astrophysical parameters of UY UMa

Parameters	Primary	Secondary
Absolute dimensions		
$M(M_\odot)$	1.151 (± 0.053)	0.237 (± 0.011)
$R(R_\odot)$	1.342 (± 0.021)	0.696 (± 0.011)
$Log\, g$ (cgs)	4.244 (± 0.024)	4.126 (± 0.024)
$\rho(\bar{\rho}_\odot)$	0.477 (± 0.031)	0.701 (± 0.047)
$a(R_\odot)$	0.416 (± 0.006)	2.026 (± 0.031)
Radiative and other parameters		
$L(L_\odot)$	1.95 (± 0.21)	0.52 (± 0.06)
V_T† (mag)	12.84 (± 0.05)	
$(B-V)_0$ (mag)	0.60 (± 0.05)	0.61 (± 0.05)
M_{bol} (mag)	3.96 (± 0.11)	5.40 (± 0.12)
BC (mag)	–0.094 (± 0.029)	–0.097 (± 0.029)
M_V (mag)	4.22 (± 0.20)	4.24 (± 0.20)
M_{V_T} (mag)	3.479 (± 0.005)	
Our distance (pc)	745 (± 17)	
GAIA distance (pc)	758.15 (± 0.02)	

† Adopted from the UCAC4 catalog (see Table 1).

GAIA's distance within the estimated error.

4. PERIOD STUDY

From our observations, seventeen times of minimum light were determined by the Kwee & van Woerden (1956) method. These appear in Table 6, together with all those that have been published since the early seven photographic timings were given by S. Beljawsky and M. Zverev (Kreiner et al. 2001). As listed in Table 6, a total of 94 times of minimum light (7 photographic, and 87 photoelectric & CCD) have been collected from a modern database (so called TIDAK; Kim et al. 2018) and recent literature.

To investigate the period variability of UY UMa, an eclipse timing diagram (ETD, traditionally called as an $(O-C)$ diagram) of the system was produced with the minima in

Table 6. Observed times of minimum light for UY UMa

JD Hel (2400000+)	Error (day)	Epoch	$(O-C_1)$ (day)	$(O-C)_{full}$ (day)	Me.†	Ty.	Ref.
25,716.344	0.06	–67,898.5	0.098	0.002	PG	II	Kreiner et al. (2001)
25,737.329	0.06	–67,842.5	0.026	–0.070	PG	II	Kreiner et al. (2001)
26,040.323	0.06	–67,037.0	0.137	0.044	PG	I	Kreiner et al. (2001)
26,093.284	0.06	–66,896.0	0.079	–0.013	PG	I	Kreiner et al. (2001)
26,450.313	0.06	–65,946.5	0.079	–0.011	PG	II	Kreiner et al. (2001)
27,307.49	-	–63,667.0	0.12	0.01	PG	I	Kreiner et al. (2001)
27,586.466	-	–62,925.0	0.092	–0.012	PG	I	Kreiner et al. (2001)
49,399.5829	0.0003	–4,914.0	0.002	–0.0014	PE	I	Hübscher et al. (1994)
49,439.4417	0.0008	–4,808.0	0.0029	–0.0006	PE	I	Hübscher et al. (1994)
49,439.6300	0.0006	–4,807.5	0.0031	–0.0003	PE	II	Hübscher et al. (1994)
49,486.4447	0.0001	–4,683.0	0.0035	0.0001	PE	I	Hübscher et al. (1994)
49,498.4776	0.0004	–4,651.0	0.0039	0.0004	PE	I	Hübscher et al. (1994)
49,776.5410	0.001	–3,911.5	0.002	–0.001	CC	II	Agerer & Hübscher (1996)
50,113.6407	0.0002	–3,015.0	0.0008	0.0001	CC	I	Agerer & Hübscher (1996)
50,142.4061	-	–2,938.5	0.0007	0.0003	CC	II	Agerer & Hübscher (1997)
50,142.5929	-	–2,938.0	–0.0005	–0.0009	CC	I	Agerer & Hübscher (1997)
50,152.3668	-	–2,912.0	–0.003	-	CC	I	Agerer & Hübscher (1997)‡
50,192.4160	-	–2,805.5	0.0002	0.0000	CC	II	Agerer & Hübscher (1997)
50,445.6650	0.001	–2,132.0	0.0008	0.0016	CC	I	Agerer & Hübscher (1998)
50,570.5012	0.0003	–1,800.0	–0.0012	–0.0002	CC	I	Agerer et al. (1999)
50,898.5770	0.0003	–927.5	–0.0015	–0.0008	CC	II	Agerer et al. (1999)
50,898.3909	0.0003	–928.0	0.0004	0.0011	CC	I	Agerer et al. (1999)
50,901.3973	0.0009	–920.0	–0.0013	–0.0007	CC	I	Diethelm(1998)
50,944.4471	0.0006	–805.5	–0.0056	-	CC	II	Agerer et al. (1999)‡
51,209.5455	0.0047	–100.5	–0.0002	–0.0005	PE	II	Agerer & Hübscher (2000)
51,236.4310	0.0003	–29.0	–0.0001	–0.0004	CC	I	Agerer & Hübscher (2000)
51,236.6203	0.0003	–28.5	0.0012	0.0009	CC	II	Agerer & Hübscher (2000)
51,246.3962	-	–2.5	0.0006	0.0003	CC	II	Yang et al. (2001)
51,247.3354	-	0.0	–0.0002	–0.0006	CC	I	Yang et al. (2001)
51,671.4867	0.0003	1,128.0	0.0023	0	CC	I	Agerer & Hübscher (2002)
51,956.5095	0.0004	1,886.0	0.0031	–0.0007	CC	I	Agerer & Hübscher (2002)
52,041.4825	0.0064	2,112.0	–0.0041	-	CC	I	Agerer & Hübscher (2002)‡
52,337.6079	0.0002	2,899.5	0.0068	0.0007	CC	II	Agerer & Hübscher (2002)
52,337.4173	0.0003	2,899.0	0.0042	–0.0019	CC	I	Agerer & Hübscher (2002)
52,369.3812	0.001	2,984.0	0.0065	0.0002	CC	I	Agerer & Hübscher (2003)

Table 6. Continued

JD Hel (2400000+)	Error (day)	Epoch	$(O-C_1)$ (day)	$(O-C)_{full}$ (day)	Me.†	Ty.	Ref.
52,408.4874	0.001	3,088.0	0.0068	0.0003	CC	I	Agerer & Hübscher (2003)
52,415.6308	0.0004	3,107.0	0.0058	–0.0007	CC	I	Samolyk (2013)
52,693.5108	0.0011	3,846.0	0.0082	–0.0002	CC	I	Diethelm (2003)
52,717.5758	0.0007	3,910.0	0.008	–0.0005	CC	I	Agerer & Hübscher (2003)
52,739.0087	-	3,967.0	0.0079	–0.0008	CC	I	Nagai (2004)
52,739.1984	-	3,967.5	0.0096	0.0009	CC	II	Nagai (2004)
52,746.5298	0.0015	3,987.0	0.0086	–0.0001	CC	I	Agerer & Hübscher (2003)
52,757.8106	0.0004	4,017.0	0.0088	0.0001	CC	I	Nelson (2004)
53,028.5463	0.0002	4,737.0	0.0113	0.0007	CC	I	Hübscher (2005)
53,110.5203	0.0042	4,955.0	0.0132	0.0021	CC	I	Hübscher (2005)
53,116.5376	0.0099	4,971.0	0.0142	0.003	CC	I	Hübscher (2005)
53,141.727	0.001	5,038.0	0.01	–0.001	CC	I	Dvorak (2005)
53,151.5066	0.0596	5,064.0	0.0135	-	CC	I	Hübscher et al. (2005)‡
53,155.4520	0.0063	5,074.5	0.0107	–0.0007	CC	II	Hübscher et al. (2005)
53,460.5966	0.007	5,886.0	0.0163	0.0029	CC	I	Hübscher et al. (2005)
53,464.5473	0.0112	5,896.5	0.0189	-	CC	II	Hübscher et al. (2005)‡
53,503.4576	0.0085	6,000.0	0.0112	–0.0025	CC	I	Hübscher et al. (2005)
53,785.8517	0.0001	6,751.0	0.0155	–0.0001	CC	I	Nelson (2007)
53,834.3601	0.0009	6,880.0	0.0175	0.0016	CC	I	Hübscher et al. (2006)
54,115.6130	0.0024	7,628.0	0.0086	-	CC	I	Hübscher (2007)‡
54,508.9394	0.0002	8,674.0	0.0197	0	CC	I	This Paper
54,509.8789	0.0003	8,676.5	0.0191	–0.0006	CC	II	This Paper
54,511.0074	0.0004	8,679.5	0.0196	–0.0001	CC	II	This Paper
54,523.9802	0.0002	8,714.0	0.0197	–0.0001	CC	I	This Paper
54,524.9211	0.0003	8,716.5	0.0206	0.0008	CC	II	This Paper
54,527.9284	0.0002	8,724.5	0.0197	–0.0001	CC	II	This Paper
54,531.3126	-	8,733.5	0.0198	–0.0001	CC	II	Nagai (2009)
54,533.1914	-	8,738.5	0.0185	–0.0014	CC	II	Nagai (2009)
54,534.1331	-	8,741.0	0.0201	0.0002	CC	I	Nagai (2009)
54,537.8926	0.0002	8,751.0	0.0195	–0.0005	CC	I	This Paper
54,538.8334	0.0002	8,753.5	0.0202	0.0003	CC	II	This Paper
54,539.0213	0.0006	8,754.0	0.0201	0.0002	CC	I	This Paper
54,570.6066	0.0003	8,838.0	0.0199	–0.0003	CC	I	Hübscher et al. (2009)
54,570.4193	0.0003	8,837.5	0.0206	0.0004	CC	II	Hübscher et al. (2009)
54,592.4164	0.0007	8,896.0	0.0206	0.0003	CC	I	Hübscher et al. (2009)
54,844.9140	0.002	9,567.5	0.0218	–0.0002	CC	II	This Paper
54,857.8866	0.0002	9,602.0	0.0217	–0.0003	CC	I	Nelson (2010)
54,863.90270	0.00031	9,618.0	0.02155	–0.00054	CC	I	This Paper
54,865.03229	0.00036	9,621.0	0.02309	0.00099	CC	I	This Paper
54,865.97095	0.00039	9,623.5	0.0217	–0.00041	CC	II	This Paper
54,866.91133	0.00019	9,626.0	0.02203	–0.00008	CC	I	This Paper
54,867.85199	0.0003	9,628.5	0.02265	0.00053	CC	II	This Paper
54,868.98090	0.00038	9,631.5	0.0235	0.00138	CC	II	This Paper
54,880.8244	0.0001	9,663.0	0.0224	0.0002	CC	I	Dvorak (2010)
54,886.8404	0.0001	9,679.0	0.0221	–0.0001	CC	I	Dvorak (2010)
54,956.4040	0.001	9,864.0	0.0223	–0.0004	CC	I	Hübscher et al. (2010)
54,957.7182	0.0005	9,867.5	0.0204	–0.0023	CC	II	Diethelm (2009)
55,235.41315	0.0004	10,606.0	0.02576	0.00095	CC	I	Brat et al. (2011)
55,262.8617	0.0003	10,679.0	0.025	–0.0001	CC	I	Dvorak (2011)
55,631.9258	0.0011	11,660.5	0.0269	–0.0013	CC	II	Diethelm (2011)
55,684.7568	0.0006	11,801.0	0.0274	–0.0014	CC	I	Diethelm (2011)
55,998.9224	0.0007	12,636.5	0.0295	–0.0022	CC	II	Diethelm (2012)
56,155.35005	0.0003	13,052.5	0.0335	0.00023	CC	II	Honkova et al. (2013)
56,355.3936	0.0023	13,584.5	0.0352	–0.0001	CC	II	Hübscher(2014)
57,025.2775	0.00007	15,366.0	0.04229	0.00003	CC	I	This Paper
57,120.4107	0.0013	15,619.0	0.0428	–0.0005	CC	I	Hübscher (2016)
57,176.4390	0.0017	15,768.0	0.0443	0.0005	CC	I	Hübscher (2016)

Table 6. Continued

JD Hel (2400000+)	Error (day)	Epoch	$(O-C_1)$ (day)	$(O-C)_{full}$ (day)	Me.†	Ty.	Ref.
57,465.4137	0.0021	16,536.5	0.0488	–0.0006	CC	II	Hübscher (2017)
57,474.4406	0.0003	16,560.5	0.0513	0.0017	CC	II	Juryšek et al. (2017)

†PG, photographic; PE, multiplier photocell; CC, electronic camera.
‡These timings were discarded in our period study because their O – C residuals show unreasonably large deviations compared with neighboring ones.

Table 6 by using YLL's light elements:

$$C_1 = \text{JD Hel } 2451247.3356 + 0^{\text{d}}.37601846E. \quad (2)$$

The upper panel in Fig. 6 shows the ETD of UY UMa where each of the timings was differentiated with different symbols according to the eclipse type and measurement methods. The $O - C_1$ residuals in the diagram, as listed in the 4th column of Table 6, reveal that the photoelectric and CCD residuals have varied in a secular period increase, which can be usually modeled in a quadratic ephemeris. In their period study, Yu et al. (2017) analyzed only the photoelectric and CCD minima available to them and derived a quadratic ephemeris:

$$O - C_1 = +0^{\text{d}}.0023(3) + 7^{\text{d}}.2(1.0) \times 10^{-7} E + 1^{\text{d}}.31(9) \times 10^{-10} E^2, \quad (3)$$

where the values in the brackets denote the standard errors of the last digit(s). Eq. (3) was drawn as the dashed curve in Fig. 6. Yu et al. (2017) excluded the earlier photographic timings in their analysis mainly because a large scatter of approximately $0^{\text{d}}.11$ in the relatively short time interval cannot reflect any real effects in the system. However, as seen in the figure, it is obvious that the earlier timings cannot be ignored in the period study of UY UMa from the point of view that the dashed curve does not match them at all. Thus, although there is a large time gap of approximately 60 yrs between the last of the earlier photographic timings and the first photoelectric one, a least-squares fit for all the $O - C_1$ residuals, including the earlier timings, was made to the quadratic ephemeris in the form of $O - C_1 = \Delta T + \Delta P + AE^2$. The resultant ephemeris was derived as follows:

$$O - C_1 = +0^{\text{d}}.0026(1) + 1^{\text{d}}.65(1) \times 10^{-6} E + 4^{\text{d}}.505(10) \times 10^{-11} E^2. \quad (4)$$

The solid line in Fig. 6 represents Eq. (4), which fits well not only for the earlier timings data but also for the recent ones overall. It is very impressive to note that the coefficient

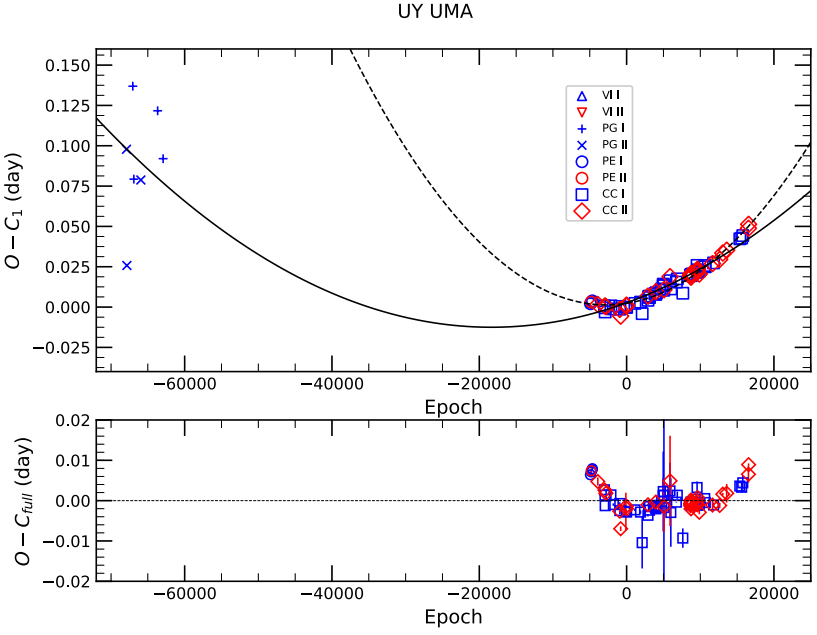

Fig. 6. Eclipse timing diagram of UY UMa constructed with Eq. (2). Timings are coded by observational method and eclipse type. The continuous and dashed curves in the upper panel were drawn based on Eqs. (3) and (4), respectively. The bottom panel shows the photoelectric and CCD residuals of the timings from Eq. (3).

of the quadratic term of Eq. (3) is approximately three times larger than that of Eq. (4). Our calculation tells us that the earlier non-photoelectric and non-CCD minima even with large observational scatters can be valuably used in constraining the size of a secular period change and thus cannot be neglected in any period studies of eclipsing binary stars, if the minima provide a longer time base in a timing history of a given eclipsing binary star.

The lower panel of Fig. 6 plots the photoelectric and CCD residuals with their error bars from Eq. (4) where the residuals without error bars have no published errors. As shown in the diagram, the photoelectric and CCD residuals clearly show some variations beyond their timing errors. To look into the details of the variations a period search (Scargle 1982) was performed with the photoelectric and CCD residuals. The six timings (2450152.3668, 2450944.4471, 2452041.4825, 2453151.5066, 2453464.5473, and 2454115.6130) were not included in the period search and the subsequent period analysis, because their residuals show unreasonably large deviations compared with neighboring ones. Each of these discarded timings is marked by an asterisk in column (8) of Table 6. Fig. 7 shows the resultant power spectra in which the two highest peaks at the periods of 10.7 yr and 23.6 yr are notably conspicuous. The longer period of 23.6 yr may not be real because it is comparable to the time-span of the times of minima except the earlier photographic ones. Nonetheless, an attempt to investigate the possible causes of the two suggested periods was made by assuming that the $O - C_1$ variations are due to combined LITEs caused by two additional bodies in the system. Thus all the $O - C_1$ residuals were fitted to the following ephemeris:

$$O - C_1 = \Delta T + \Delta P + AE^2 + \tau_3 + \tau_4, \quad (5)$$

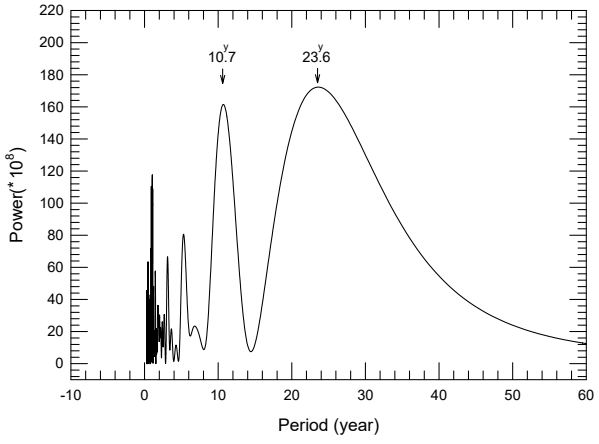

Fig. 7. Power spectra of the photoelectric and CCD residuals from Eq. (4).

where τ_3 and τ_4 are the LITEs due to the hypothetical 3rd and 4th bodies, respectively. The parametric and differential forms of the orbital elements of a given light-time orbit were adopted from Irwin (1952, 1959). Iterative least-squares fits of the $(O - C)_1$ residuals to Eq. (5) were made with the Levenberg-Marquardt method (Press et al. 1992), which was frequently used in the period studies of some other stars (Kim et al. 2005, 2014, 2018). In the calculations, each of timings was given a weight equal to an inverse value of each of their published (see Table 6) or assigned errors. For the photographic and CCD minima with no published errors, the error for the former minima was given as $0^d.06$ based on their scatters and for the latter ones $0^d.0019$, the average value of the published errors of the photoelectric and CCD minima. The calculations converged quickly to yield the solution listed in Table 7 wherein the parenthesized entries give the standard deviations of the tabulated quantities. The $O - C_1$ residuals were again plotted in the top of Fig. 8 where the solid and dashed curves represent the full and quadratic terms in Eq. (5) and Table 7, respectively. In the 2nd and 3rd parts of the figure the contributions to light times by the third and fourth bodies are plotted, respectively. At the bottom of the figure, the $(O - C)_{full}$ residuals from the full ephemeris of Eq. (5), which appear in the fifth column of Table 6, are plotted. As shown in Fig. 8, the residuals from the observed times of minimum light follow the theoretical light time curves due to the assumed third and fourth bodies very well. As listed in Table 7, the semi-amplitude, orbital period, and eccentricity for the light time orbit of the mass center of the eclipsing pair due to the third and fourth bodies are ($0^d.0026$, $12^y.02$, and 0.448) and ($0^d.0083$, 46^y 27, and 0.449), respectively. Interestingly, the eccentricity of the third body is practically the same as that of the fourth one. In addition, the minimum masses corresponding to the

Table 7. Orbital elements of light time orbits suggested for UY UMa system

Element	Value	
ΔT_0 (day)	0.0058 (17)	
ΔP (day)	0.00000214 (18)	
T_0 (JD Hel)	2451247.3414 (17)	
P (day)	0.37602060 (18)	
A (day/cycle)	$5.23\,(31) \times 10^{-11}$	
	Third body (j = 3)	**Fourth body (j = 4)**
$a_{12} \sin(i_j)$ (AU)	0.45 (18)	1.45 (56)
K_j (day)	0.0026 (9)	0.0083 (29)
e_j	0.45 (12)	0.45 (36)
ω_j (deg)	86 (12)	111 (12)
T_j (JD Hel)	2453586 (192)	2448183 (155)
P_j (year)	12.02 (1.54)	46.3 (7.37)
$M_{j\,\min}$ ($M_\odot$)	0.11 (1)	0.16 (1)

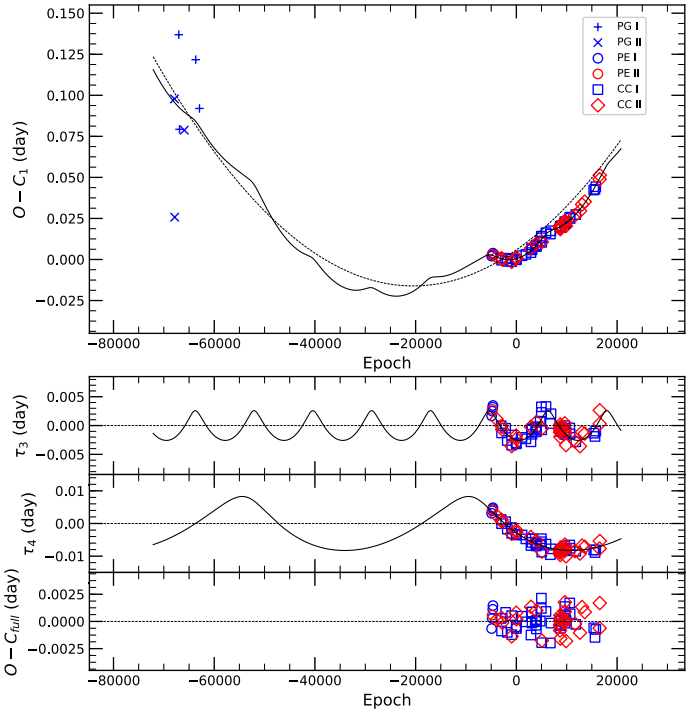

Fig. 8. Eclipse timing diagram of UY UMa constructed with Eq. (2). Each of the timings is coded by observational method and eclipse type. The dashed and solid curves in the upper panel are drawn with only the quadratic and full terms in Eq. (5), respectively. In the 2nd and 3rd panels the contributions to light times by the third and fourth bodies, respectively, are plotted. The bottom panel shows the residuals of the timings from Eq. (5).

third and fourth bodies are calculated to be $M_3 = 0.11\ M_\odot$ and $M_4 = 0.16\ M_\odot$, respectively. Furthermore, it is noticed that there may exist a commensurable relation between the orbital periods: $77P_3 = 20P_4$.

The parabolic component of the period change of UY UMa gives the secular period increase rate of $1.02(60) \times 10^{-8}$ d/yr, implying the secular mass transfer rate of almost $2.68(26) \times 10^{-8}\ M_\odot$/yr from the less massive to the more massive star if the mass and angular momentum of the system are conserved.

5. CONCLUSIONS

In general, there are two competing theories that explain why the orbital period of an eclipsing binary system changes regularly: one is the LITE by a third object, and the other is the Applegate model (Applegate 1992). The latter explains that the cyclic change is caused by the gravitational coupling of the orbit to variation in the shape of a magnetically active component. This model requires changes in the luminosity and differential rotation of the active star at the levels of $\Delta L/L \simeq 0.1$ and $\Delta\Omega/\Omega \simeq 0.01$, respectively. Thus, the two cyclical changes found in the UY UMa system may be caused by one of three possible mechanisms: (a) LITEs due to two additional objects, as discussed in the previous section, (b) Applegate models operating simultaneously on two magnetic active components, or (c) the combination of the LITE due to a third object and the Applegate model working on a magnetically active component. For UY UMa the (b) option seems unlikely because of the thin convective zone of the small star, which is supported by Mullan's (1975) conclusion that there should be dark spots preferentially on the more massive components of W UMa-type contact binary systems. We calculated the Applegate model parameters, as listed in Table 8, under the assumption that the two cyclical changes are caused by the more massive components. In the calculation, the mass of the convective shell is assumed to be 10% of the stellar mass. The rms luminosity changes ($\Delta L_{\rm rms}$) converted to magnitude scale in Table 8 were obtained with Eq. (4) in the paper of Kim et al. (1997). As listed in Table 8, the Applegate model parameters, especially $\Delta L/L$ and $\Delta\Omega/\Omega$, for the two period modulations are one or two orders of magnitude less than the nominal ones suggested by Applegate (1992), indicating that the Applegate mechanism does not work in the UY UMa system.

Table 8. Model parameters of magnetic activity for UY UMa

Model parameter	Period modulation		Unit
	12.0 year	46.3 year	
ΔP	0.1209	0.1003	sec
$\Delta P/P$	3.72×10^{-6}	3.09×10^{-6}	–
ΔJ	7.96×10^{46}	6.60×10^{46}	g cm^2/s
I_s	1.33×10^{54}	2.00×10^{54}	g cm^2
$\Delta\Omega/\Omega$	3.09×10^{-4}	1.71×10^{-4}	–
ΔE	9.52×10^{39}	4.37×10^{39}	erg
ΔL_{rms}	7.89×10^{31}	9.39×10^{30}	erg
	2.06×10^{-2}	2.45×10^{-3}	$L_\odot$
	1.06×10^{-2}	1.26×10^{-3}	L_p
Δm_{rms}	± 0.0091	± 0.0011	mag
B	6.97×10^3	3.24×10^3	gauss

Thus, we concluded that two periodic changes were most likely caused by LITEs due to two outer objects orbiting the eclipsing pair. In this case, the minimum masses of the third and fourth bodies are calculated to be 0.11 $M_\odot$ and 0.16 $M_\odot$, respectively. Our hypothesis of circumbinary objects may be supported by the third lights detected in our light curve synthesis. As shown in Table 4, the additional bodies seems to emit more energy in shorter wavelengths. This indicates that at least one of them may be an early-type star.

Recently, Yang & Qian (2015 ; hereafter YQ) made a statistical analysis of 45 deep, low mass ratio (DLMR) overcontact binaries of which the mass ratio and the fill-out factor are less than 0.25 and larger than 50%, respectively. They found some statistical relationships among the various physical parameters: q *vs.* f, q *vs.* J_{spin}/J_{orb}, log $(M/M_\odot)$ *vs.* log $(L/L_\odot)$, and log $(M/M_\odot)$ *vs.* log $(R/R_\odot)$ where q, f, J_{spin}, J_{orb}, M, L, and R represent mass ratio, fill-out factor, spin angular momentum, orbital angular momentum, mass, luminosity, and radius, respectively. After their study, Şenavci et al. (2016) studied 25 Kepler eclipsing binaries of W UMa-type showing total eclipses and presented their precise orbital solutions as well as their absolute dimensions. The derived mass ratios of all Kepler binaries are less than 0.18 and 15 out of 25 systems have fill-out factors larger than 50%.

We investigated the statistical relations found by YQ by using the physical parameters of UY UMa and the Kepler overcontact binaries. The relations of q – f, q – J_{spin}/J_{orb}, log$(M/M_\odot)$ – log$(L/L_\odot)$, and log$(M/M_\odot)$ – log$(R/R_\odot)$ are shown from Figs. 9-11, respectively. The dotted lines in red in all figures denote the relations given by YQ. The solid lines in blue are derived by us. Fig. 9 shows the diagram of q – f in which the black line represents f = 50%. In the diagram, we see that the Kepler overcontact binaries show large deviations from the YQ equation (f (%) = 117.6 – 527.6 × q + 1164.9 × q^2), indicating that the YQ relationship between q and f is very weak and thus the YQ's minimum mass ratio of

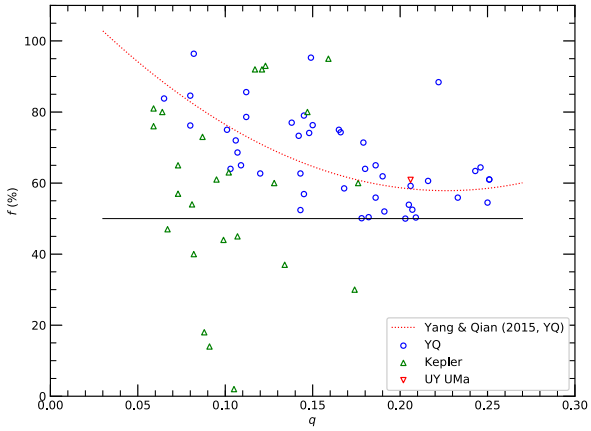

Fig. 9. Relationship of q – f. The dotted line in red represents Eq. (1) in the paper of Yang & Qian (2015, hereafter YQ). The solid line denote f = 50%. The Kepler overcontact binaries show large deviations from the relationship.

q_{min} = 0.44 derived from the relation may deviate somewhat from the actual value.

To investigate the relation of q – J_{spin}/J_{orb}, we calculated J_{spin}/J_{orb} with the equation given by YQ and Li & Zhang (2006) as follows:

$$\frac{J_{spin}}{J_{orb}} = \frac{1+q}{q}\left(k_1^2 r_1^2 + k_2^2 r_2^2 q\right), \quad (6)$$

where $r_{1,2}$ and $k_{1,2}$ are the relative and gyration radii for both components, respectively. We adopted $k_1^2 = k_2^2 = 0.05$, which is the value used by YQ. In equation (3) of the YQ paper, it is pointed out that $q/(1+q)$ is a typo error of $(1+q)/q$. The top panel of Fig. 10 shows the relation of q – J_{spin}/J_{orb} and the dotted curve represents the YQ relation (J_{spin}/J_{orb} = 0.5104 – 3.7738 × q + 8.2817 × q^2). The dotted horizontal line represents J_{spin}/J_{orb} = 1/3, at which a tidal instability called Darwin instability (Darwin 1879; Hut 1980) starts. In the middle panel, the residuals from the YQ relation are plotted and show a quasi-sinusoidal pattern, indicating that the YQ equation does not represent J_{spin}/J_{orb} = well as a function of q. It has been well known that J_{spin}/J_{orb} = of W UMa-type contact binaries is strongly correlated with the mass ratio q, but a direct polynomial relation between them is difficult to obtain (Li & Zhang 2006). To obtain a good expression of the relationship between q and J_{spin}/J_{orb}, we adopted a new equation as follows,

$$\frac{J_{spin}}{J_{orb}} = \frac{1+q}{q}\left(a_0 + a_1 \times q + a_2 \times q^2\right). \quad (7)$$

An iterative least-squares method was used to fit the data

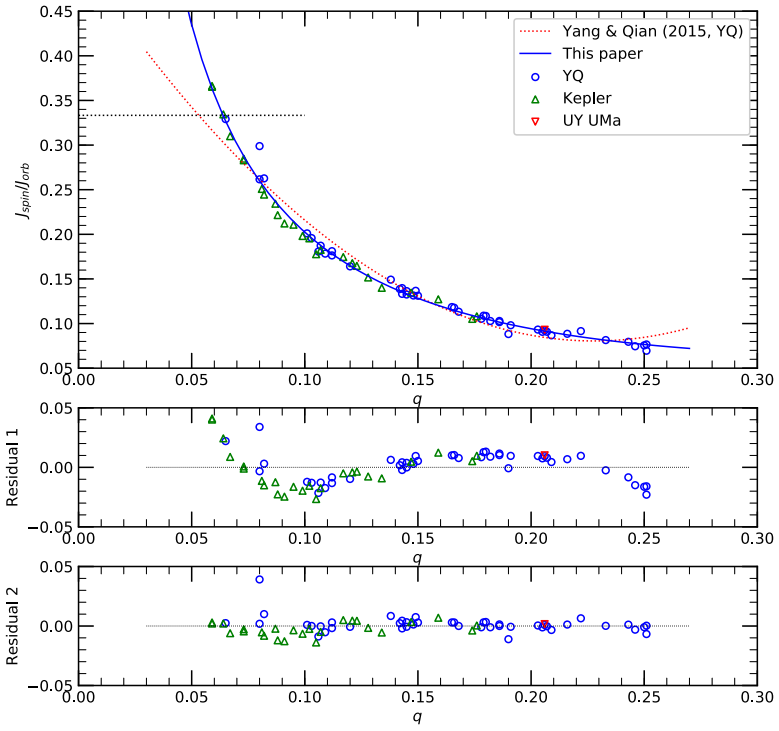

Fig. 10. Top: Relationship of $q - J_{spin}/J_{orb}$. The dotted line in red represents Eq. (4) in the paper of YQ. The solid line in blue represents Eq. (6). Middle: The residuals from the YQ equation. Bottom: The residuals from Eq. (6) (see the text).

set of q and J_{spin}/J_{orb} to the above equation. The result is a_0 = 0.0236 (± 0.0006), a_1 = –0.0651 (± 0.0094), and a_2 = 0.127 (± 0.034). The solid curve in the top panel represents Eq. (7) with the derived coefficients and gives a satisfactory fit to the observed systems which is also evidenced by the residuals from Eq. (7) in the bottom panel. In addition, we numerically solved Eq. (7) for q by setting J_{spin}/J_{orb} = 1/3 and obtained a minimum mass ratio of q_{min} = 0.064 for the observed systems, which is larger than YQ's value of 0.053 but smaller than approximately 0.076 – 0.078 of Li & Zhang (2006).

Finally, the mass-luminosity (M – L) and mass-radius (M – R) diagrams in log scale are shown in the left and right panels of Fig. 11, respectively. In the diagrams, the zero age main-sequence (ZAMS) and terminal age main-sequence (TAMS) taken from the Padova stellar evolution model with solar abundance (Girardi et al. 2000), are drawn as the solid and dotted lines in black, respectively. In addition, the dotted lines in red and blue are drawn with the linear relations determined by YQ and the authors, respectively. For comparison, we listed the coefficients of the linear equations of log ($L/L_\odot$) and log ($R/R_\odot$) as functions of log ($M/M_\odot$) in Table 9. In the M – L and M – R diagrams, the primary star of UY UMa occupies the middle position of the main sequence band, and the secondary star is at the bottom of the subgiant zone. However, in the M – L diagram, the primary components of the Kepler binary stars are mostly below ZAMS and most of the secondary components are located in the upper part of the subgiant region. Moreover, in the M – R diagram, the primary stars are aligned along the middle down the main sequence band while most secondary stars are in the upper part of the subgiant region.

In this paper, we presented and analyzed new *BVRI* CCD light curves of UY UMa, including the first red and infrared observations. No O'Connell effect was found in our light curves with a long-duration totality (approximately 43^m) at secondary eclipse. The physical parameters derived from the light curve synthesis are totally different from ones suggested by Yang et al. (2001): UY UMa is an A-subtype over-contact binary with a low mass ratio of q = 0.21, a high inclination of 81°.4, a small temperature difference of ΔT = 18°, a large fill-out factor of f = 0.61, and a third light of approximately 10% of the total systemic light. The absolute dimensions of the system were determined as follows: M_1 = 1.15 $M_\odot$, M_2 = 0.24 $M_\odot$, R_1 = 1.34 $R_\odot$, R_2 = 0.70 $R_\odot$, L_1 = 1.95 $L_\odot$, and L_2 = 0.52 $L_\odot$. The ETD based on all available times of minima, including our seventeen new timings, shows

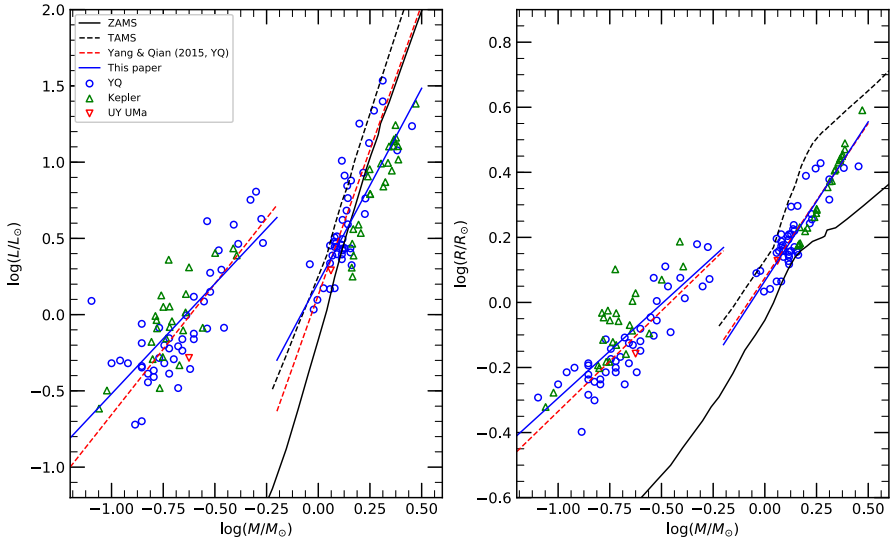

Fig. 11. Left: Relation of log ($M/M_{\odot}$) – log ($L/L_{\odot}$). Right: Relation of log ($M/M_{\odot}$) – log ($R/R_{\odot}$).

Table 9. Linear relations of log ($L/L_{\odot}$) and log ($R/R_{\odot}$) with respect to log ($M/M_{\odot}$)

Coefficient	YQ		This paper	
	Primary	Secondary	Primary	Secondary
	$\log(L/L_{\odot}) = a_0 + a_1 \log(M/M_{\odot})$			
a_0	0.1282(58)†	1.0618(128)	0.211(44)	0.926(105)
a_1	3.8083(35)	1.7179(184)	2.547(197)	1.445(148)
	$\log(R/R_{\odot}) = a_0 + a_1 \log(M/M_{\odot})$			
a_0	0.0751(14)	0.2826(35)	0.066(11)	0.285(36)
a_1	0.9513(86)	0.6177(50)	0.978(48)	0.579(51)

†In Eq. (6) of Yang & Qian (2015), the value is written as 1.1282, which is a typo error of 0.1282.

that the orbital period of UY UMa has experienced complex variation for 60^{y} since 1929^{y}. The variations in the orbital period were decoupled into two cyclically varying terms with periods of $12^{y}.0$ and $46^{y}.3$ and a secularly increasing term with the rate of $1.02(60) \times 10^{-8}$ d/yr. The latter may be interpreted to be due to a conservative mass transfer of $2.68 \times 10^{-8} M_{\odot}$/yr from the secondary component to the primary one. Two competing theories (LITE and Applegate model) as the possible causes of two cyclical changes of period were tested. The Applegate mechanism may not work in the UY UMa system because the Applegate model parameters, especially $\Delta L/L$ and $\Delta\Omega/\Omega$, for the two period modulations are one or two of magnitude less than the nominal ones suggested by Applegate (1992). However, the third lights detected in our light curve synthesis may support the LITEs due to two outer objects. Currently, we have concluded that the two periodic changes were most likely caused by LITEs due to two circumbinary objects orbiting the eclipsing pair. The calculated minimum masses of the third and fourth bodies are 0.11 $M_{\odot}$ and 0.16 $M_{\odot}$, respectively, which seem to emit more energy in shorter wavelengths. Finally, YQ's statistical relations among the physical parameters of 45 DLMR contact binaries were revisited by using the physical parameters of UY UMa and 25 Kepler contact binaries provided by Şenavci et al. (2016). The minimum mass ratio was newly determined as q_{min} = 0.064 by using a new equation describing J_{spin}/J_{orb} as a function of q. In addition, the evolutionary status of UY UMA and 25 Kepler contact binaries based on the M – L and M – R diagrams shows that both components of UY UMa occupy positions in the diagrams similar to other DLMR stars, although Kepler stars are located differently from the positions occupied by other DLMR stars.

ACKNOWLEDGMENTS

We would like to thank the staff of the LOAO and SOAO for assistance with our observations. Our thanks also go to the anonymous referees for their careful corrections.

We have used the SIMBAD database operated by the Centre de Donnees Astronomiques (Strasbourg). This work was supported by the grants 2017R1A4A1015178 and 2018R1D1A1A09081827 from the National Research Foundation of Korea (NRF).

ORCID

Chun-Hwey Kim https://orcid.org/0000-0001-8591-4562
Mi-Hwa Song https://orcid.org/0000-0003-2772-7528
Jang-Ho Park https://orcid.org/0000-0001-9339-4456
Min-Ji Jeong https://orcid.org/0000-0002-6927-7572
Hye-Young Kim https://orcid.org/0000-0002-6687-6318
Chengho Han https://orcid.org/0000-0002-2641-9964

REFERENCES

Agerer F, Dahm M, Hübscher J, Photoelectric minima of selected eclipsing binaries and maxima of pulsating stars, Inf. Bull. Var. Stars 4712, 1-5 (1999).

Agerer F, Hübscher J, Photoelectric minima of selected eclipsing binaries, Inf. Bull. Var. Stars 4383, 1-4 (1996).

Agerer F, Hübscher J, Photoelectric minima of selected eclipsing binaries and maxima of pulsating stars, Inf. Bull. Var. Stars 4472, 1-4 (1997).

Agerer F, Hübscher J, Photoelectric minima of selected eclipsing binaries and maxima of pulsating stars, Inf. Bull. Var. Stars 4562, 1-4 (1998).

Agerer F, Hübscher J, Photoelectric minima of selected eclipsing binaries and maxima of pulsating stars, Inf. Bull. Var. Stars 4912, 1-5 (2000).

Agerer F, Hübscher J, Photoelectric minima of selected eclipsing binaries and maxima of pulsating stars, Inf. Bull. Var. Stars 5296, 1-16 (2002).

Agerer F, Hübscher J, Photoelectric minima of selected eclipsing binaries, Inf. Bull. Var. Stars 5484, 1-12 (2003).

Applegate JH, A mechanism for orbital period modulation in close binaries, Astrophys. J. 385, 621-629 (1992). https://doi.org/10.1086/170967

Binnendijk L, The orbital elements of W Ursae Majoris systems, Vistas Astron. 12, 217-256 (1970). https://doi.org/10.1016/0083-6656(70)90041-3

Brat L, Trnka J, Smelcer L, Lehky M, Kucakova H, et al., B.R.N.O. contributions #37 - times of minima, Open Eur. J. Var. Stars 137, 1-57 (2011).

Darwin GH, A tidal theory of the evolution of satellites, The Observatory 3, 79-84 (1879).

Diethelm R, Notes on BG Boo, BS Cas, BW Cas, V520 Cas, WW Eri, KQ Gem, IX Mon, DZ Ori, WY Per, GQ Tau, UY UMa, BBSAG Bull. 117, 9 (1998).

Diethelm R, 162-nd List of minima timings of eclipsing binaries by BBSAG observers, Inf. Bull. Var. Stars 5438, 1-11 (2003).

Diethelm R, Timings of minima of eclipsing binaries, Inf. Bull. Var. Stars 5894, 1-10 (2009).

Diethelm R, Timings of minima of eclipsing binaries, Inf. Bull. Var. Stars 5992, 1-22 (2011).

Diethelm, R, Timings of minima of eclipsing binaries, Inf. Bull. Var. Stars 6029, 1-22 (2012).

Drilling JS, Landolt AU, Normal Stars, in Allen's Astrophysical Quantities, 4th ed., ed. Cox AN (Springer-Verlag, New York, 2000), 381-396.

Dvorak SW, Times of minima for neglected eclipsing binaries in 2004, Inf. Bull. Var. Stars 5603, 1-3 (2005).

Dvorak SW, Times of minima for eclipsing binaries 2009, Inf. Bull. Var. Stars 5938, 1-3 (2010).

Dvorak SW, Times of minima for eclipsing binaries 2010, Inf. Bull. Var. Stars 5974, 1-2 (2011).

Flower PJ, Transformations from theoretical Hertzsprung-Russell diagrams to color-magnitude diagrams: effective temperatures, B-V colors, and bolometric corrections, Astrophys. J. 469, 355-365 (1996). https://doi.org/10.1086/177785

Girardi L, Bressan A, Bertelli G, Chiosi C, Evolutionary tracks and isochrones for low-and intermediate- mass stars: from 0.15 to 7 M_{sun}, and from Z = 0.0004 to 0.03, Astron. Astrophys. Suppl. Ser. 141, 371-383 (2000). https://doi.org/10.1051/aas:2000126

Guthnick P, Prager R, Benennung von veränderlichen Sternen, Astron. Nachr. 6017, 251-257 (1934). https://doi.org/10.1002/asna.19342511702

Hambálek L, Pribulla T, The reliability of mass-ratio determination from light curves of contact binary stars, Contrib. Astron. Obs. Skalnate Pleso 43, 27-46 (2013).

Hoňková K, Juryšek J, Lehký M, Šmelcer L, Trnka J, et al., B.R.N.O. contributions #38 times of minima, Open Eur. J. Var. Stars 160, 1-174 (2013).

Hübscher J, Photoelectric Minima of selected eclipsing binaries and maxima of pulsating stars, Inf. Bull. Var. Stars 5643, 1-20 (2005).

Hübscher J, Photoelectric minima of selected eclipsing binaries and maxima of pulsating stars, Inf. Bull. Var. Stars 5802, 1-14 (2007).

Hübscher J, BAV Results of observations - photoelectric minima of selected eclipsing binaries and maxima of pulsating stars, Inf. Bull. Var. Stars 6118, 1-17 (2014).

Hübscher J, BAV-Results of observations - photoelectric minima of selected eclipsing binaries, Inf. Bull. Var. Stars 6157, 1-11 (2016).

Hübscher J, BAV-Results of observations - photoelectric minima of selected eclipsing binaries and maxima of pulsating stars, Inf. Bull. Var. Stars 6196, 1-27 (2017).

Hübscher J, Agerer F, Frank P, Wunder E, Bundesdeutsche Arbeitsgemeinschaft für Veränderliche Sterne e.V. (BAV): Beobachtungsergebnisse, BAV Mitt. 68, 1-24 (1994).

Hübscher J, Lehmann PB, Monninger G, Steinbach HM, Walter F, BAV-results of observations - photoelectric minima of selected eclipsing binaries and maxima of pulsating stars, Inf. Bull. Var. Stars 5918, 1-16 (2010).

Hübscher J, Paschke A, Walter F, Photoelectric minima of selected eclipsing binaries and maxima of pulsating stars, Inf. Bull. Var. Stars 5657, 1-24 (2005).

Hübscher J, Paschke A, Walter F, Photoelectric minima of selected eclipsing binaries and maxima of pulsating stars, Inf. Bull. Var. Stars 5731, 1-31 (2006).

Hübscher J, Steinbach HM, Walter F, BAV-results of observations - photoelectric minima of selected eclipsing binaries and maxima of pulsating stars, Inf. Bull. Var. Stars 5874, 1-13 (2009).

Hut P, Stability of tidal equilibrium, Astron. Astrophys. 92, 167-170 (1980).

Irwin JB, The determination of a light-time orbit, Astrophys. J. 116, 211-217 (1952). https://doi.org/10.1086/145604

Irwin JB, Standard light-time curves, Astron. J. 64, 149-155 (1959). https://doi.org/10.1086/107913

Jeong MJ, Kim CH, The first comprehensive photometric study of the neglected binary system V345 Cassiopeiae, J. Astron. Space Sci. 30, 213-221 (2013). https://doi.org/10.5140/JASS.2013.30.4.213

Juryšek J, Hoňková K, Šmelcer L, Mašek M, Lehký M, et al., B.R.N.O. contributions #40 times of minima, Open Eur. J. Var. Stars 179, 1-145 (2017).

Kim CH, Kim HW, Park JH, Song, MH, Jeong MJ, et al., New CCD times of minima of 17 eccentric eclipsing binary systems, Inf. Bull. Var. Stars 6202, 1-3 (2017).

Kim CH, Jeong JH, Demircan O, Müyesseroğlu Z, Budding E, The period changes of YY Eridani, Astron. J. 114, 2753-2763 (1997).

Kim CH, Kreiner JM, Zakrzewski B, Ogłoza W, Kim HW, et al., A comprehensive catalog of galactic eclipsing binary stars with eccentric orbits based on eclipse timing diagrams, Astrophys. J. Suppl. Series 235, 41 (2018). https://doi.org/10.3847/1538-4365/aab7ef

Kim CH, Nha IS, Kreiner JM, A possible detection of a second light-time orbit for the massive, early-type eclipsing binary star AH Cephei, Astron. J. 129, 990-1000 (2005). https://doi.org/10.1086/426747

Kim CH, Song MH, Yoon JN, Han W, Jeong MJ, BD Andromedae: a new short-period RS CVn eclipsing binary star with a distant tertiary body in a highly eccentric orbit, Astrophys. J. 788, 134 (2014). https://doi.org/10.1088/0004-637X/788/2/134

Kreiner JM, Kim CH, Nha IS, An Atlas of (O-C) Diagrams of Eclipsing Binary Stars (Press of Pedagogical Univ., Krakow, Poland, 2001).

Kurucz RL, New atmospheres for modelling binaries and disks, in Light Curve Modeling of Eclipsing Binary Stars, ed., Milone EF (Springer-Verlag, New York, 1993), 93.

Kwee KK, van Woerden H, A method for computing accurately the epoch of minimum of an eclipsing variable, Bull. Astron. Inst. Neth. 12, 327-330 (1956).

Lee JW, Youn JH, Kim CH, Lee CU, Kim HI, A photometric study of the short-period close binary V432 Persei and its implications for the star's evolution, Astron. J. 135, 1523-1532 (2008). https://doi.org/10.1088/0004-6256/135/4/1523

Li L, Zhang F, The dynamical stability of W Ursae Majoris-type systems, Mon. Not. R. Astron. Soc. 369, 2001- 2004 (2006). https://doi.org/10.1111/j.1365-2966.2006.10462.x

Mullan DJ, On the possibility of magnetic starspots on the primary components of W Ursae Majoris type binaries, Astrophys. J. 198, 563-573 (1975). https://doi.org/10.1086/153635

Nagai K, Visual and CCD minima of eclipsing binaries during 2003, Var. Star Bull. Jpn. 42, 1-7 (2004).

Nagai K, Visual and CCD minima of eclipsing binaries during 2008, Var. Star Bull. Jpn. 48, 1-11 (2009).

Nelson RH, CCD Minima for selected eclipsing binaries in 2003, Inf. Bull. Var. Stars 5493, 1-6 (2004).

Nelson RH, CCD Minima for selected eclipsing binaries in 2006, Inf. Bull. Var. Stars 5760, 1-6 (2007).

Nelson RH, CCD Minima for selected eclipsing binaries in 2009, Inf. Bull. Var. Stars 5929, 1-4 (2010).

O'Connell DJK, The so-called periastron effect in close eclipsing binaries, Riverview College Observatory Publications, vol. 2, no. 6 (1951).

Odell AP, Eaton JA, López-Cruz O, V432 Per, a close binary star in poor thermal contact, Mon. Not. R. Astron. Soc. 400, 2085-2089 (2009). https://doi.org/10.1111/j.1365-2966.2009.15600.x

Press W, Flannery BP, Teukolsky SA, Vetterling WT, Numerical Recipes (Cambridge Univ. Press, Cambridge, 1992).

Samolyk G, Recent minima of 273 eclipsing binary stars, J. Am. Assoc. Var. Star Obs. 41, 122-133 (2013).

Scargle JD, Studies in astronomical time series analysis. II. Statistical aspects of spectral analysis of unbevenly spaced data, Astrophys. J. 263, 835-853 (1982). https://doi.org/10.1086/160554

Şenavci HV, Doğruel MB, Nelson RH, Yilmaz M, Selam SO, Precise orbital solutions for KEPLER eclipsing binaries of W UMa type showing total eclipses, Publ. Astron. Soc. Aust. 33,

e043 (2016). https://doi.org/10.1017/pasa.2016.39

Terrell D, Wilson RE, Photometric mass ratios of eclipsing binary stars, Astrophys. Space Sci. 296, 221-230 (2005). https://doi.org/10.1007/s10509-005-4449-4

Tody D, The IRAF data reduction and analysis system, in 1986 Astronomy Conferences, Tucson, AZ, 13 Oct 1986. https://doi.org/10.1117/12.968154

Torres G, Andersen J, Giménez A, Accurate masses and radii of normal stars: modern results and applications, Astron. Astrophys. Rev. 18, 67-126 (2010). https://doi.org/10.1007/s00159-009-0025-1

Van Hamme W, New limb-darkening coefficients for modeling binary star light, Astron. J. 106, 2096-2117 (1993). https://doi.org/10.1086/116788

Van Hamme W, Wilson RE, Stellar atmospheres in eclipsing binary models, ASP Conf. Ser. 298, 323-328 (2003).

Wilson RE, Eccentic orbit generalization and simultaneous solution of binary star light and velocity curves, Astrophys. J. 234, 1054-1066 (1979). https://doi.org/10.1086/157588

Wilson RE, Accuracy and efficency in the binary star reflection effect, Astrophys. J. 356, 613-622 (1990). https://doi.org/10.1086/168867

Wilson RE, Biermann P, TX Cancri - which component is hotter?, Astron. Astrophys. 48, 349-357 (1976).

Wilson RE, Devinney EJ, Realization of accurate close-binary light curves: application to MR Cygni, Astrophys. J. 166, 605-619 (1971). https://doi.org/10.1086/150986

Yang Y, Liu Q, V432 Persei: A contact binary with compoenents in poor thermal contact, Astron. J. 123, 443-449 (2002). https://doi.org/10.1086/324642

Yang Y, Liu Q, Leung KC, UY Ursae Majoris: A W-subtype W UMa system with a small mass ratio, Astron. Astrophys. 370, 507-512 (2001). https://doi.org/10.1051/0004-6361:20010261

Yang YG, Qian SB, Deep, low mass ratio overcontact binary systems. XIV. A statistical snalaysis of 46 sample binaries, Astron. J. 150, 69 (2015). https://doi.org/10.1088/0004-6256/150/3/69

Yu YX, Zhang XD, Hu K, Xiang FY, Orbital period variations of two W UMa-type binaries: UY UMa and EF Boo, New Astron. 55, 13-16 (2017). https://doi.org/10.1016/j.newast.2017.02.002

Zacharias N, Finch CT, Girard TM, Henden A, Bartlett JL, et al., The fourth US Naval observatory CCD astroghaph catalog (UCAC4), Astron. J. 145, 44 (2013). https://doi.org/10.1088/0004-6256/145/2/44